

STABILITY OF CONCENTRATION WAVES IN GASEOUS POLLUTANT TRACE DYNAMICAL ADSORPTION

Alain Perrard and Jean-Pierre Joly, Université de Lyon, Université Lyon1, CNRS, UMR 5256, Institut de recherches sur la catalyse et l'environnement de Lyon,

2 avenue Albert Einstein, F-69626 Villeurbanne Cedex, France

A. Joly, Université de Lyon, Université Lyon1, CNRS, UMR 5258, Institut Camille Jordan,

43 boulevard du 11 novembre 1918, F-69622 Villeurbanne Cedex, France

Abstract

The mechanism of dynamical adsorption of single vapors (including VOC's and water) in activated carbon beds generally involves a transport step from the gaseous phase to the surface of carbon, followed by an equilibrium of adsorption. Numerical simulations at constant temperature and constant flow rate, described in a previous work (Carbon 2006, Aberdeen), illustrated the fact that the behavior of the pollutant concentration front, which builds into the carbon bed, is strongly dependent upon the adsorption isotherm chosen to model the phenomenon. In the present work, a uniform mathematical treatment, using the linear driving force approximation, is presented along with a simple mathematical condition for the building of a constant pattern concentration front. Implications to popular simple breakthrough models used in the field of vapor dynamical adsorption are discussed.

Keywords: Numerical modeling, dynamic adsorption, finite elements

Introduction

Environmental concerns promote the interest for the capture of Volatile Organic Compounds (VOC's) by flowing contaminated air through activated carbon beds. Interesting models in this field consider an adsorption mechanism involving a mass-transfer controlling step, followed by an adsorption state at equilibrium. With respect to the kinetics of adsorption, a linear driving force approximation is usually used (Gluckauf and Coates 1947; Clark 1987; Malek and Farooq 1997; Sircar and Hufton 2000; Lorimier *et al.* 2005; Manjare and Ghoshal 2006). The isotherm of adsorption is chosen to at best represent the property of the considered pollutant-adsorbent couple. In a previous work (Perrard *et al.* 2006), numerical simulations with various isotherms led to a variety of breakthrough curves differing mainly by the existence or not of a constant pattern solution. The aim of this paper is to present the condition that the isotherm expression has to fulfill for a constant pattern concentration front to exist. Finite element simulations allow us to illustrate how this front is approached starting from different initial conditions.

The model

Figure 1 shows the propagation of the pollutant concentration front through the carbon bed. In this figure, c , c_0 , t and x denote the pollutant concentration in the gas phase, this concentration at bed inlet, time and abscissa in bed, respectively.

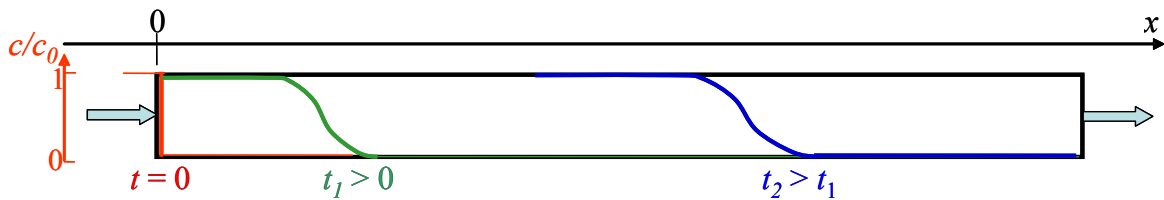


Figure 1. Propagation of the concentration front $c/c_0 = f(x,t)$ through the adsorbent bed

The material balance over a differential element of the adsorbent bed volume leads to:

$$-F \frac{\partial c}{\partial x} = \rho_b S \frac{\partial W}{\partial t} + \alpha S \frac{\partial c}{\partial t} \quad (1)$$

where F , ρ_b , S , W and α denote the total gas flow rate, the apparent density of the adsorbent bed, its section area, the amount of adsorbate per unit mass of adsorbent and the void volume fraction of the adsorbent bed, respectively.

For trace adsorption modeling, the last term in Eq. (1) may be omitted. Consequently, in the following, this mass balance is written:

$$-F \frac{\partial c}{\partial x} = \rho_b S \frac{\partial W}{\partial t} \quad (2)$$

On the other hand, the adsorption rate is written (Linear driving force approximation):

$$\frac{\partial W}{\partial t} = k_T (c - c_s) \quad (3)$$

where k_T and c_s denote a proportionality constant and the pollutant concentration in the gas phase at the external surface of the adsorbent, respectively.

Now, a general expression for the isotherms is:

$$\Theta = \frac{W}{W_0} = f(c_s) \quad (4)$$

where W_0 is the value of W with $c_s = c_0$.

Extracting c_s from Eq. (4), one obtains:

$$c_s = f^{-1}(\Theta) \quad (5)$$

Then, the variables Θ , c , x and t are changed for the dimensionless variables U , C , X and T , respectively, according to the equations shown in Table 1.

Table 1. Dimensionless variables.

$U = 1 - \Theta$	$C = \frac{c}{c_0}$	$X = \frac{k_T \rho_b W_0 S}{F} x$	$T = k_T c_0 t$
------------------	---------------------	------------------------------------	-----------------

Introducing these dimensionless variables in Eqs. (2) and (3), the following system of two partial differential equations (PDE) is obtained:

$$\begin{cases} \frac{\partial C}{\partial X} - \frac{\partial U}{\partial T} = 0 & (6) \\ \frac{\partial U}{\partial T} + C = g(U) & (7) \end{cases}$$

where the expression of $g(U)$, related to the chosen isotherm, is such as:

$$g(0) = 1, \quad g(1) = 0 \quad (8)$$

The resolution of this system with convenient initial and boundary conditions provides the concentration front and the breakthrough curve.

Constant pattern front

Concentration front displacement rate

For an observer traveling at the speed of the adsorption front, this front is immobile and consequently he observes a stationary counter-flow of gas and of solid. The mass balance on an element of the adsorption front, where the pollutant concentration is c and the amount of adsorbate per unit mass of adsorbent is W , is written as:

$$\frac{c}{c_0} = \frac{W}{W_0} = \Theta \text{ or } C = 1 - U \quad (9)$$

Considering Eqs. (6) and (9) and using the Euler circular equation:

$$\left(\frac{\partial C}{\partial T}\right)_X = -\left(\frac{\partial C}{\partial X}\right)_T \left(\frac{\partial X}{\partial T}\right)_C \quad (10)$$

one achieves the very interesting conclusion that the speed v of front traveling is constant, whatever C , and given by:

$$v = \frac{dX}{dT} = 1 \quad (11)$$

Constant pattern front existence

Assuming a progressive concentration wave towards the abscissa x increasing such as:

$$\left\{ \begin{array}{l} U(X, T) = U(\tilde{X}) \\ C(X, T) = C(\tilde{X}) \end{array} \right. \quad (12)$$

$$\quad (13)$$

with $\tilde{X} = X - vT$, and the boundary conditions:

$$T \rightarrow -\infty \Leftrightarrow C \rightarrow 1 \Leftrightarrow U \rightarrow 0 \quad (14)$$

$$T \rightarrow +\infty \Leftrightarrow C \rightarrow 0 \Leftrightarrow U \rightarrow 1 \quad (15)$$

Moreover, the variables C and U are continuously monotonous such as:

$$\frac{dC}{d\tilde{X}} < 0 \quad \text{and} \quad \frac{dU}{d\tilde{X}} > 0 \quad (16)$$

Then, given $v = 1$ after Eq. (11), the system of two PDE (6) and (7) becomes:

$$\left\{ \begin{array}{l} \frac{dC}{d\tilde{X}} = -\frac{dU}{d\tilde{X}} \\ \frac{dC}{d\tilde{X}} + C = g(U) \end{array} \right. \quad (17)$$

$$\quad (18)$$

Thus, by integrating Eq. (17) and owing to Eq. (14) or (15), one recovers Eq. (9) characteristic of a constant pattern concentration front. On the other hand, taking into account Eqs. (9) and (16), Eq. (18) leads to the necessary and sufficient condition for a constant pattern front to exist:

$$g(U) < 1 - U \quad \text{for} \quad 0 < 1 - U < 1 \quad (19)$$

Application to Freundlich model

The Freundlich model is based on the following isotherm equation:

$$W = K_F c_s^{\frac{1}{n}} \quad (20)$$

where K_F is a constant and n is the *Freundlich slope* higher than 1 in the practical applications. This isotherm reduces to the linear isotherm for $n = 1$.

Using the dimensionless variables defined in Table 1, the system of PDE (6) and (7) provides:

$$\begin{cases} \frac{\partial C}{\partial X} - \frac{\partial U}{\partial T} = 0 \\ \frac{\partial U}{\partial T} + C = (1 - U)^n \end{cases} \quad (6) \quad (21)$$

It is clear that $g(U) = (1 - U)^n$ is smaller than $1 - U$ if and only if $n > 1$, for $0 < 1 - U < 1$.

Finite element simulations

Simulations of concentration fronts and of breakthrough curves for the model involving the driving force approximation and the isotherm of Freundlich were carried out with Consol Software. Figures 2 and 3 show the concentration fronts along the carbon bed and the corresponding breakthrough curves for different times and bed lengths, respectively. The value of n was set to 1.5. As predicted by the theory, the concentration front issued from a concentration step at the bed inlet reaches a constant pattern front for a sufficient bed length. The constant shape solutions have been established by Clark (Clark 1987)

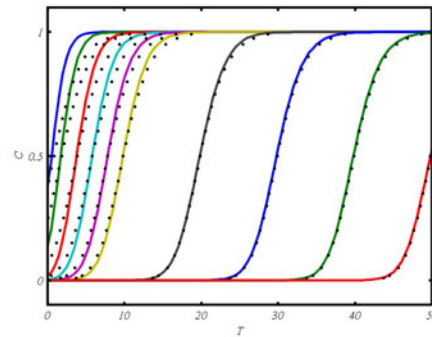
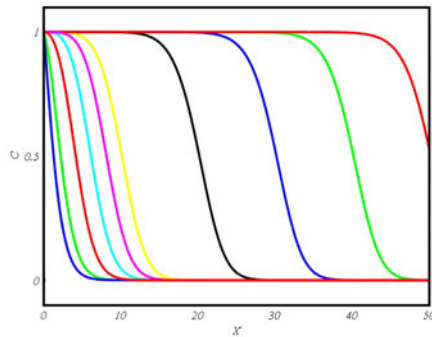
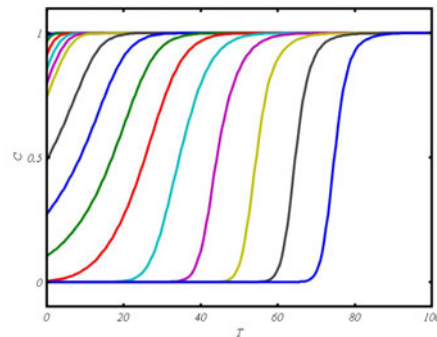
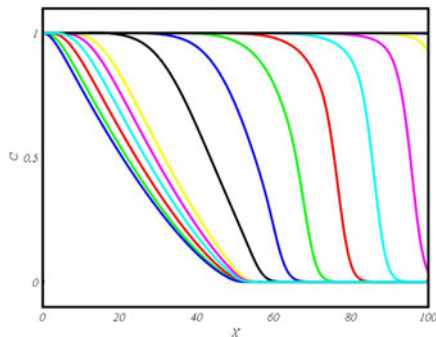


Figure 2. Transfer + Freundlich ($n=1.5$). Concentration front issued from an initial concentration step at consecutive times: $T=1, 2, 4, 6, 8, 10, 20, 30, 40, 50$.

Figure 3. Transfer + Freundlich ($n=1.5$). Breakthrough curve, corresponding to Figure 2, for bed lengths $X=1, 2, 4, 6, 8, 10, 20, 30, 40, 50$. Dots represent the constant pattern solution (Clark model).

Figures 4 and 5 show the results of simulations with the same model but with a different initial condition where the concentration C in the bed is represented by a decreasing line, the slope of which is smaller than that of the constant pattern front at its inflexion point. In this initial condition, U is chosen equal to $1 - C$. This is the

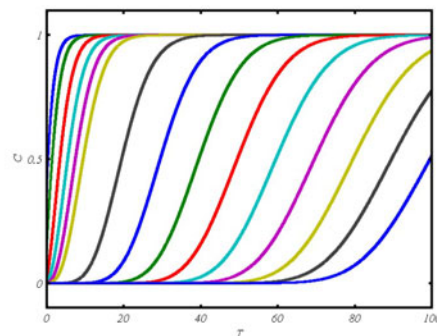
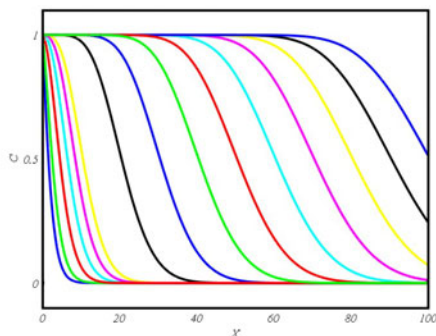
case of a self-sharpening wave, the concentration front going once again to the constant pattern solution for a sufficient bed length. These results are in agreement with those of the wave theory in chromatography (Helfferich and Carr 1993).



<p>Figure 4. Transfer + Freundlich ($n = 1.5$). Concentration front issued from a small slope initial front (Self sharpening wave) at consecutive times: $T=1, 2, 4, 6, 8, 10, 20, 30, 40, 50, 60, 70, 80$.</p>	<p>Figure 5. Transfer + Freundlich ($n = 1.5$). Breakthrough curve corresponding to Figure 4, for bed lengths: $X=1, 2, 4, 6, 8, 10, 20, 30, 40, 50, 60, 70, 80, 90, 100$.</p>
---	---

Figures 6 and 7 show simulations carried out with the same model, but for $n = 1$, i.e., a linear isotherm. As predicted by the theory, which rules out a constant pattern solution for this value of n , the slope of the concentration front steadily decreases with the length of the adsorbent bed.

The same kind of simulations has been carried out with linear driving force models involving the isotherms of Langmuir, of Type V and of Dubinin-Astakhov. It can be easily shown that the model involving a Langmuir isotherm always possesses a constant pattern solution and that such a solution does not exist when the Type V isotherm is used. The model of Dubinin-Astakhov may lead to both cases. In addition, in a previous work we showed that constant pattern breakthrough times are close to those predicted by the famous Wheeler-Jonas model for small values of the outlet concentration, i.e., at the very beginning of pollutant breakthrough.



<p>Figure 6. Transfer + Freundlich ($n = 1$). Concentration front issued from an initial concentration step at consecutive times: $T=1, 2, 4, 6, 8, 10, 20, 30, 40, 50, 60, 70, 80, 90, 100$.</p>	<p>Figure 7. Transfer + Freundlich ($n = 1$). Breakthrough curve, corresponding to Figure 6, for bed lengths: $X=1, 2, 4, 6, 8, 10, 20, 30, 40, 50, 60, 70, 80, 90, 100$.</p>
---	--

Potential practical application to breakthrough curves

Organic vapors

The adsorption isotherms $\Theta = f(c_s)$ of organic vapors are represented by curves with a downward concavity, for instance that of Langmuir (Vahdat 1997), that of Freundlich (Tsai *et al.* 1999) or that Duninin-Astakhov (D-A) with sufficiently large value of the parameter ε :

$$\Theta = K \exp \left[- \left(\frac{1}{\varepsilon} \ln \frac{c_\infty}{c_s} \right)^N \right] \quad (22)$$

where K , c_∞ and ε are constant parameters. Eq.(22) with $N = 2$ has been extensively used to predict adsorption capacities for vapors (Wood 1992; Cal *et al.* 1997).

These isotherms satisfy Eq. (19), which means that a constant pattern front establishes in the linear driving force model. Besides, at the very beginning of the breakthrough, external transport would be determining for the adsorption rate and conveniently described by linear driving force approximation. The consequence is that breakthrough times for a small fraction of the inlet concentration obey the model of Wheeler-Jonas (Wheeler and Robell 1969; Jonas and Rehrmann 1973). This argument could help to understand why the model of Wheeler-Jonas is convenient for so many applications (Lodewyckx *et al.* 2004). In contrast other popular parented models (Mecklenburg 1925; Yoon and Nelson 1984) implicitly imply the non-existence of a constant pattern pollutant concentration front.

Water vapor

Water vapor adsorption equilibrium on hydrophobic carbons may be described by isotherms showing an upward concavity, for instance Type V or D-A (Stoeckli 1998) with a small value of the parameter ε . In this case Eq. (19) is not fulfilled and, consequently, no constant pattern breakthrough curve is expected. Figure 8 shows the result of a simulation obtained with the linear driving force approximation accompanied by a D-A isotherm:

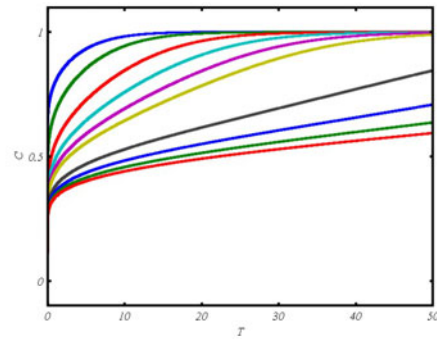
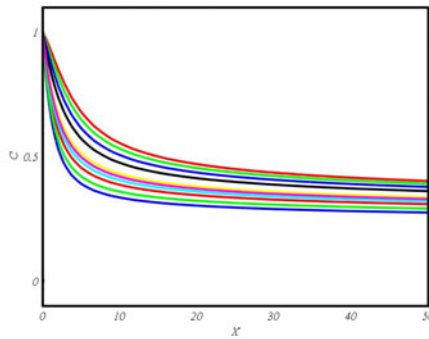


Figure 8. Transfer + D-A ($N = 3$, $\varepsilon = 1$, $K = 2.16$).
Concentration front issued from an initial
concentration step at consecutive times:
 $T = 1, 2, 4, 6, 8, 10, 20, 30, 40, 50$.

Figure 9. Transfer + D-A ($N = 3$, $\varepsilon = 1$, $K = 2.16$).
Breakthrough curve, corresponding to Figure 8, for bed
lengths
 $X = 1, 2, 4, 6, 8, 10, 20, 30, 40, 50$.

It is seen that the breakthrough is immediate. The curves presented in Figures 8 and 9 qualitatively recall recent experimental results on water concentration fronts (Lodewyckx *et al.* 2006a) or on breakthrough through activated carbon beds (Lodewyckx *et al.* 2006b). The approach adopted in the present work could provide some clues to explain such results.

Conclusion

This paper presents an examination of the behavior of the concentration front in dynamical adsorption of vapor traces through carbon beds. The considered mechanism of adsorption involves a mass-transfer controlling step, followed by an adsorption state at equilibrium. This mass-transfer is modeled by means of the linear driving force approximation and the adsorption equilibrium is characterized by various isotherms. Numerical simulations of the pollutant concentration front and of the corresponding breakthrough curve are carried out by the finite element method. The existence of a constant pattern concentration front (a progressive concentration wave), for a sufficient bed length, depends on the chosen isotherm. A simple mathematical condition for the existence of such a front, only involving the intrinsic properties of the isotherm, is presented. This front is closely approached either by a self-widening wave or a self-sharpening wave according to the initial conditions about the pollutant concentration and adsorbent coverage within the carbon bed. When this mathematical condition is not met, the width of the concentration front increases with the bed length. Some simple equations proposed in the literature to model the breakthrough of vapors through carbon beds implicitly involve the existence of a constant pattern concentration front and others do not. An interesting particular case is that of Dubinin-Astakhov isotherm with smaller values of the energy parameter, i.e., with an upward concavity, which results in a concentration front and breakthrough curve qualitatively recalling amazing experimental results, recently published, on water dynamic adsorption on hydrophobic activated carbons.

References

- Cal, M. P., Rood, M. J., and Larson, S. M. 1997. *Gas phase adsorption of volatile organic compounds and water vapor on activated carbon cloth*. Energy & Fuels **11** (2):311-315.
- Clark, R. M. 1987. *Evaluating the cost and performance of field-scale granular activated carbon systems*. Environmental Science and Technology **21** (6):573-580.
- Gluckauf, E., and Coates, J. I. 1947. *Theory of chromatography. Iv. The influence on incomplete equilibrium on the front boundary of chromatograms and on the effectiveness of separation*. Journal of the Chemical Society:1315-1321.
- Helfferich, F. G., and Carr, P. W. 1993. *Nonlinear-waves in chromatography .I. Waves, shocks, and shapes*. Journal of Chromatography **629** (2):97-122.
- Jonas, L. A., and Rehrmann, J. A. 1973. *Predictive equations in gas adsorption kinetics*. Carbon **11** (1):59-64.
- Lodewyckx, P., Blacher, S., and Leonard, A. 2006a. *Use of x-ray microtomography to visualise dynamic adsorption of organic vapour and water vapour on activated carbon*. Adsorption **12** (1):19-26.
- Lodewyckx, P., Wood, G. O., and Ryu, S. K. 2004. *The wheeler-jonas equation: A versatile tool for the prediction of carbon bed breakthrough times*. Carbon **42** (7):1351-1355.
- Lodewyckx, P., Wullens, H., Léonard, A., Blacher, S., Crine, M., Mafalda Ribeiro, A., and Loureiro, J. M. 2006b. *Study of the dynamics of water adsorption on activated carbon by a combination of high-resolution x-ray microtomography and breakthrough measurements*. Paper read at The International Conference on Carbon 2006, at Aberdeen (Scotland). CD: *Extended Abstracts* ISBN: 0-9553365-1-1.
- Lorimier, C., Subrenat, A., Le Coq, L., and Le Cloirec, P. 2005. *Adsorption of toluene onto activated carbon fibre cloths and felts: Application to indoor air treatment*. Environmental Technology **26** (11):1217-1230.
- Malek, A., and Farooq, S. 1997. *Kinetics of hydrocarbon adsorption on activated carbon and silica gel*. Aiche Journal **43** (3):761-776.
- Manjare, S. D., and Ghoshal, A. K. 2006. *Studies on adsorption of ethyl acetate vapor on activated carbon*. Industrial & Engineering Chemistry Research **45** (19):6563-6569.
- Mecklenburg, W. 1925. *Layer filtration, a contribution to the theory of the gas mask*. Zeitschrift fuer Elektrochemie und Angewandte Physikalische Chemie **31**:488-495.
- Perrard, A., Joly, A., and Joly, J. P. 2006. *About equations used to model single gas dynamic adsorption onto activated carbon beds*. Paper read at The International Conference on Carbon 2006, at Aberdeen (Scotland). CD: *Extended Abstracts*. ISBN: 0-9553365-1-1.
- Sircar, S., and Hufton, J. R. 2000. *Why does the linear driving force model for adsorption kinetics work?* Adsorption-Journal of the International Adsorption Society **6** (2):137-147.
- Stoeckli, F. 1998. *Recent developments in dubinin's theory*. Carbon **36** (4):363-368.
- Tsai, W. T., Chang, C. Y., Ho, C. Y., and Chen, L. Y. 1999. *Adsorption properties and breakthrough model of 1,1-dichloro-1-fluoroethane on activated carbons*. Journal of Hazardous Materials **69** (1):53-66.
- Vahdat, N. 1997. *Theoretical study of the performance of activated carbon in the presence of binary vapor mixtures*. Carbon **35** (10-11):1545-1557.

- Wheeler, A., and Robell, A. J. 1969. *Performance of fixed-bed catalytic reactors with poison in the feed*. Journal of Catalysis **13** (3):299-305.
- Wood, G. O. 1992. *Activated carbon adsorption capacities for vapors*. Carbon **30** (4):593-599.
- Yoon, Y. H., and Nelson, J. H. 1984. *Application of gas adsorption kinetics. I. A theoretical model for respirator cartridge service life*. American Industrial Hygiene Association Journal (1958-1999) **45** (8):509-516.